Effect and consequence of the rheological properties of nano Fe$_2$O$_3$-modified drilling muds in the Dibella oil field

Abdoulaye seyni Mahamadou[1,2]*, Gu Jun[1] and
Maimouna Issa Moctar[1]

[1]Key Laboratory of Tectonics and Petroleum Resources, Ministry of Education, China Faculty of Earth
Resources, China University of Geosciences, Wuhan, China, [2]China University of Geosciences, Earth
Sciences Department, Drilling and Cement Completion Laboratory, Wuhan, China

The development of supportable, cost-effective, and high-performance
nanoparticles (NPs) is one of the new examination points within penetrating
applications. The consideration of tailorable nanoparticles offers the chance to
figure out water-based drilling fluids (WBDFs) with upgraded properties,
providing exceptional opportunities in the energy, oil, gas, water, or
framework enterprises. In WBDFs, nano and micron materials are investigated
to control their rheological properties and their influence. This paper aims to
analyze the influence of nano Fe$_2$O$_3$ on the rheological behavior of drilling fluid
muds under high temperatures and pressure. Additionally, we seek to identify the
optimal concentration of iron oxide nanoparticles that maintain consistent
rheology; we examined the interfering effects of shear rates and iron oxide
nanoparticle temperature on the shear type of the changed depleting liquid in the
Dibella oil field to make the penetrating activity efficient, realistic, and skilled. We
observe that as the temperature increases, the water-based mud (WBM), plastic
viscosity (PV), yield point (YP), and gel strength (Gs) decrease until the reject
structure is disrupted. Therefore, we must proceed with our assessment using
nano Fe$_2$O$_3$ to resolve the shortcomings of the slope framework. Six water-based
mud cakes containing 0.5, 1, 1.5, 2, 2.5, and 3 g weight percent of iron oxide
(Fe$_2$O$_3$) nanoparticles were prepared for this evaluation. The experimental
outcomes revealed an optimal nanoparticle mixing of 2.5 g weight percent,
which resulted in a 13.8% reduction in the API filtrate volume and a 40%
reduction in filter cake thickness. At 300°F temperature and type
10.00 pressure, the results of our experiments consistently demonstrate a
decrease of 14.77% in the rheological properties of PV and YP and 10 s and
10 min in the gel strength of carbon oxide nanoparticles. The YP−PV span is 2.7,
and the yield strength is 11 lb/100 ft^2. On the other hand, mud cake A, which
contains 0.5 wt% NPs, loses 6 mL of fluid after 30 min. In contrast, drilling mud
cake E, which is composed of 3 wt% NPs, shows a fluid loss of 5.1 mL in the API
filter press test. Based on the Bingham plastic model, the maximum shear stress
versus shear rate was observed for bentonite drilling muds E and F, with 2.5 wt%
and 3 wt% NPs, respectively, and this result indicates that the use of nano Fe$_2$O$_3$
can effectively adjust the properties of drilling fluids.

KEYWORDS

drilling fluids, high pressure, high temperature, shear stress, nano Fe$_2$O$_3$, rheological
properties, Dibella oil field

1 Introduction

The superior itemizing and planning plan of the exhausting fluid system is the best approach to showing the objective significance of the hydrocarbon vault. Drilling fluids, such as oil-based muds (OBMs) and water-based drilling fluids (WBDFs), are primarily used to drain oil and gas wells. They have demonstrated a sophisticated method of handling the acting of rheological characteristics under various crippling conditions (Hamed and Belhadri, 2009; Livescu, 2012). WBDFs are widely used among these weakening liquids and are regarded as unassuming and inoffensive to the biological structure (Christiansen, 1991; Rodrigues et al., 2006; Tehrani et al., 2009; Mao et al., 2015a; Sadeghalvaad and Sabbaghi, 2015). Nevertheless, it has also been declared that massive extension, restricted application, and polymer-added material may give rise to concerns regarding unstable rheological characteristics under downhole circumstances of high pressure and high temperature (HPHT) (Abdo and Haneef, 2013; Abdo et al., 2014; Mao et al., 2015a). The oil and gas industry generally views the increase in potassium chloride (KCl) in WBDFs as a means of better hydration blockage and control over rheological qualities, particularly in shale (Khodja et al., 2010). At high temperatures and high pungency circumstances, the rheology and filtration characteristics of exhausting muds with water-dissolvable polymers alter the working conditions (Vermolen et al., 2011). Nanoparticles (NPs) have been added to water-set-up mud works to address the viscoelastic and thixotropic properties of water-based mud (WBM), thereby improving the rheological congruity of penetrating muds (Aadnoy and Chenevert, 1987; Coussot et al., 2004; Le Guen et al., 2009). Riley et al. (2012) assessed the utilization of silica nanomaterials in water-based fluids (WBFs) to further develop the restraint of shale materials and compared it with an engineered-based mud, which is regularly utilized for wellbore soundness concerns in shale arrangements. The example with 3 wt% of silica exhibited a penetrability decrease of 20.1%, which is more prominent than the base example without silica, showing its capacity to fit and seal miniature pores and miniature breaks. Abduo M. I. et al. (2016) experimented with bentonite particles with a molecule size between 4 and 9 nm as an added substance to WBFs and then contrasted the outcomes and programming interface bentonite properties with an example with neighborhood bentonite not at a nanosize. The rheological properties like AV, PV, and YP diminished because of the expansion of bentonite with nanosize distances across, as the solid substance of the liquid was diminished. When it comes to controlling the rheological properties of depleting fluids, Mao et al. (2015b); Jain et al. (2015) recommended using nanocomposites as an alternative to soils and polymers. They are used to fight against the difficulties brought on by the intense heat and pressure of the more important course of action due to the warm defilement of the mud sections when entering mud. To modify the rheological properties and shale hindrance of water-based muds, harmful mud additives such as multi-walled carbon nanotubes (MWCNTs), graphene nanoplatelets, and nano-silica were added by Aftab et al. Their results showed that GNP can be used as an overlay option to improve the execution of WBM (Ismail et al., 2016). The utilization of nanoparticles in the oil business will permit

penetrating designers to change the rheology of the boring liquid by changing the arrangement (Abdo and Haneef, 2012). Nanoparticles can work on the rheological qualities of drilling fluids utilizing different instruments that fundamentally rely upon the consistent period of penetrating liquids and the attributes of the nanoparticles (Brady and Brady, 1983; Jain et al., 2015; Taraghikhah et al., 2015). This advancement in the consistency of nanofluids can be assessed by utilizing homogeneous, strong liquid connection models (Singh et al., 2011). Laszlo et al. (2001) fixed modified emulsion drilling fluids under HPHT conditions using soil and silica nanoparticles (Laszlo et al., 2001). They found that either separately or in combination, nanosoil and nanosilica can immobilize or modify emulsions that enter fluids. Both thickness and yield strength are improved when the additional iron oxide particles in the bentonite liquid become more centrally distributed (Nasser et al., 2013). The progress of drilling mud is significant because it increases oil recovery and reduces the time expected to get the principal oil (Nagre et al., 2014). The rheological elements of a drilling mud can be prepared by many variables during the boring activity, such as temperature, pressure (which is a component of boring profundity), and impurities (Khoshakhlagh et al., 2012). According to some theories, nano Fe_2O_3 can significantly affect compressive strength, flexural strength, and controllable splitting strength by up to 5% at particular easing times (Rashad, 2013). The cementitious material's convenience, setting time, mechanical strength, water retention, and durability were all improved by the nano iron oxide (Fe_2O_3) (Nelson et al., 1990). The gel structure gives adequate consistency to allow for an increase in the water content of the substance without allowing free water (Akhtarmanesh et al., 2013). Mahmoud et al. (2019) found that to lessen porousness and liquid intrusion, the base colloidal silica NP fixation should be 10 wt%, and a superior stopping execution was noted with the 35 nm measured NPs when contrasted with the 50 nm NPs. Then again, water-based liquids are widely utilized for boring applications because of their minimal expense, easy handling, and no imperative removal, as well as their environmental friendliness compared to oil-based fluids (OBFs) (Li et al., 2019). A polyacrylamide (PAM)-based copolymer was utilized to upgrade the shale security of delicate shale developments in the penetrating system (Aramendiz and Imqam, 2019). A few nanoparticles were utilized to upgrade the shale restraint properties, like nano-silica (Ma et al., 2020), multi-walled carbon nanotubes (Rana et al., 2020), graphene (Bayat and Shams, 2019; Mady et al., 2020), and iron oxide (Du et al., 2019). Nanomaterials are utilized in concrete formulations to build their durability and strength (Esmaeili et al., 2011; Sikora et al., 2018). Nanomaterials have many applications in various areas of petroleum engineering, like investigation, boring, and production (Mohamadian et al., 2018). NPs have higher surface area-to-volume ratios than larger particles. This characteristic provides them with several advantages, including greater strength, improved electrical and thermal properties, and increased chemical reactivity (Godson et al., 2010). NPs added to the drilling fluid can help fill the gaps between particles and reduce the void space in the mud cake. This prevents fluid from flowing from the borehole into the formation. Various types of nanoparticles, including ZnO, montmorillonite, carbon nanotubes, SiO_2, nanoclay, nanographite, TiO_2, Fe_2O_3, graphene, calcium oxide, CuO, and Al_2O_3, have been introduced into drilling fluid to improve fluid loss control and rheology (Al-

Saba et al., 2018). Mohammed (2017) conducted a study to examine the impact of Fe_2O_3 nanoparticles of two different sizes (3 and 30 nm) on the rheological and filtration properties of bentonite-based drilling fluids (BBDFs) under HPHT conditions. The study found that the smaller nanoparticles had a greater effect on increasing the plastic viscosity (PV) and yield point (YP) than the larger NPs. In another study, researchers observed that by varying the concentration of silica nanoparticles in the WBM from 0.001 to 1.5 wt%, the viscosity of the drilling mud increased (Gbadamosi et al., 2019). Cheraghian et al. (2015) demonstrated that incorporating nanoclay into PAM had a beneficial impact on the viscosity characteristics of the polymer solution. In recent years, there has been a great interest in improving the stability of polymers through the modification of their structure or by using NPs (Hu et al., 2017). To improve control over rheological properties and maintain thermal stability, the market has introduced activated weighting agents, thermally stable clay, and fluid systems with temperature and contaminant tolerance. These polymers provide filtration and rheological properties, as well as high thermal stability. Ongoing research aims to identify the micro-mechanisms of rheology at high temperatures (Ezell and Harrison, 2008). Fe_2O_3 NPs impart a positive charge to the bentonite–water suspension, thereby enhancing shear stresses at all shear rates (Rezaei et al., 2020). The use of NPs significantly improved the thermal stability of hydrolyzed polyacrylamide (HPAM) over a 12-day test period. In other words, the effective viscosity was approximately five times higher at a 0.8 wt% NP loading (Haruna et al., 2019). The studies conducted by Harounal Maje confirm that the dispersion formed by SMag-NP-PAM showed higher viscosity and better mobility control. Additionally, it exhibited a lower contact angle and interfacial tension (IFT) than pure SMag-NPs, PAM, and IO-NP-PAM under high-temperature, high-salinity (HTHS) conditions (Fakher et al., 2020). Two possible schemes have been proposed to explain the phenomenon of decreased viscosity. The first scheme involves the formation of carboxylic acid groups on the PAM backbone. This leads to a reaction with hydroxyl groups on the CQDs, resulting in the formation of ester bonds. The second scheme suggests that long macromolecular chains in the PAM are broken down into smaller chains. The CQDs can protonate the carboxylate groups in the PAM, converting them from –COO– to –COOH. This increases the acidity of the polymer and eventually causes a conformational transition, changing the polymer from a stretched state to a coiled state (Haruna et al., 2019). Polymer injection is an enhanced oil recovery (EOR) method that improves mobility control. It is used to increase oil recovery beyond what can be achieved through primary and secondary production mechanisms (Nourafkan et al., 2019). HTHS and extreme pH conditions can have a significant impact on the stability of polymers and degrade their performance in EOR (Caenn et al., 2011). The presence of MWCNTs significantly increased the viscosity of polymer solutions compared to pure co/terpolymer solutions (Geehan et al., 1989). In this study, we tested and quantified the sensing and rheological properties of drilling mud modified with nano Fe_2O_3 at different temperatures. We used the shear stress *versus* shear rate variation for analysis. The objective of measuring fluid control was to enhance the cost-effectiveness, safety, and profitability of drilling operations.

2 Experimental apparatus instruments

For our experiments, we utilized specific equipment to perform various tasks. We employed a Hamilton Beach Mixer to effectively mix the components, a filtration loss tester to accurately measure the filtration loss, a six-speed viscometer to calculate the rheological properties, a Chinese brand kSW Muffle Furnace for calcining the dry fluid sludge, a Thermo Fisher Scientific Apreo S Scanning Electron Microscope (SEM) to analyze the samples, and an XPert PRO MPD X-ray Diffractometer to examine the X-ray diffraction (XRD) of the six mud cakes. Figure 1 displays the instruments that were utilized for our experiments.

3 Experimental process

Bentonite is extensively used to control some characteristics of incoming fluids that are clear-cut, like facilitating cutting movement to the surface, breaking up oil emulsions, and applying hydrostatic tension in the wellbore (Al-Yasiri and Al-Sallami, 2015). Bentonite's capacity to restrict, tighten, and constantly drain fluid enhances its control over fluid flow in permeable systems (Khalil and Mohamed Jan, 2012). For this reason, we implanted 22.5 g of organophilic soil bentonite to improve uniformity throughout the graded chamber. We utilized organophilic bentonite to demonstrate significant thixotropic or aging behavior, which is utilized in various applications. This thixotropic behavior is connected to its physical properties, specifically swelling and delamination behavior, as well as heterogeneous charge behavior that impacts particle shape. We added 350 mL of freshwater to help decay the excess debris. Using an electric blender, the contents in the bucket were blended until there were no more projections. We added 0.5 weight percent, 1 weight percent, and 1.5 weight percent NPs and then 2 weight percent, 2.5 weight percent, and 3 weight percent NPs after 16 h of supporting the damaged fluid in suspension. The pursuit of consistent rheology is essential when selecting the rate and insertion of iron oxide. By incorporating the specified quantity, we have successfully achieved a desirable rheological constant. Following a 2-min electric blender homogenization and persistent mixing of the fluid tests, Figure 2 displays the assessment affiliation, and Figure 3 displays the six mud cakes made with varying concentrations of iron oxide (Fe_2O_3) nanoparticles. The materials utilized in the underlying cycle are provided in Table 1.

3.1 Synthesis of iron oxide (Fe_2O_3) nanoparticles

The synthetic precipitation strategy was decided to incorporate iron oxide (Fe_2O_3) nanoparticles. We degraded 5 g of ferric chloride hexahydrate ($FeCl_3.6H_2O$) in 100 mL of demineralized water. The products were then cleaned and rinsed with ethanol and deionized water to eliminate the overflow base. It was dried in a hot air stove for 2 hours at 100°C after some time had passed. After that, the object was sliced into pieces, which were calcined for 4 hours at 450°C in a cover. Eventually, the XRD revealed the bronzed natural-hued hematite powder content, with the development we anticipated to complete the SEM.
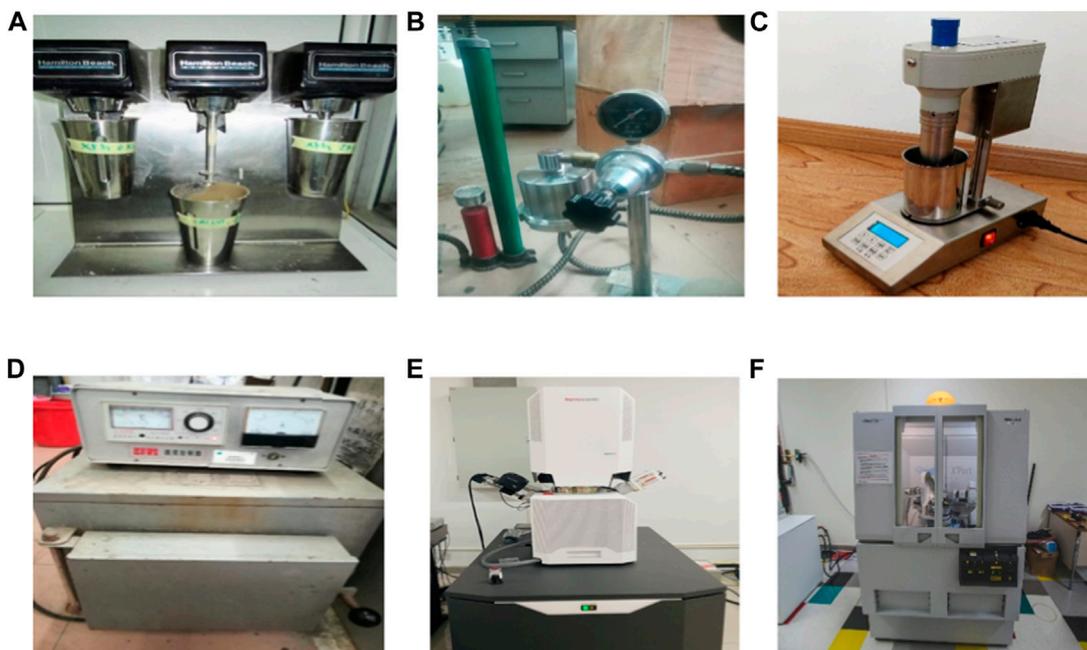
FIGURE 1
Experiment machine tools. Hamilton Beach Mixer; filtration loss tester; six-speed viscometer ; Chinese Brand kSW Muffle Furnace; Thermo Fisher Scientific Apreo S; XPert PRO MPD X-ray Diffractometer **(A–F)**.
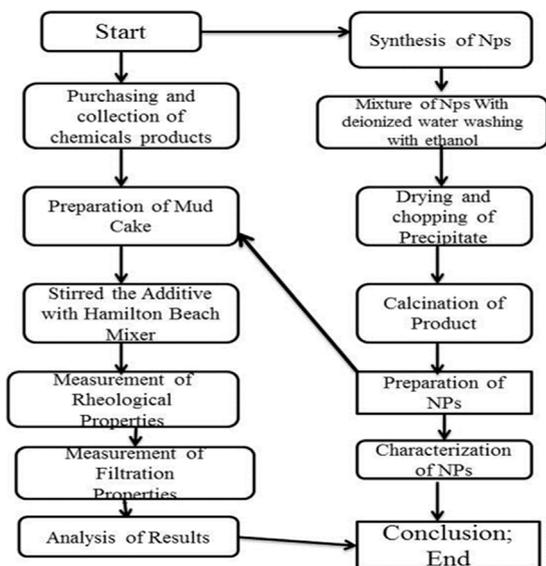

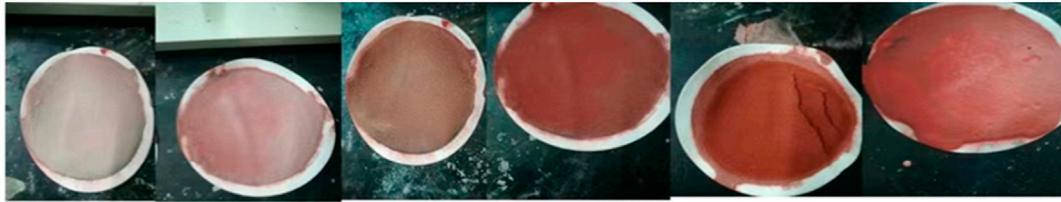**FIGURE 2**
Flowchart of the experimental process.

3.2 Rheological measurements

Rheological investigation plays a crucial role in the polymer-flooding process. To achieve the best possible oil recovery, it is important to accurately determine the viscosity of the polymer. This allows for a favorable mobility ratio between the oil and displacing fluid. However, it is worth noting that the viscosity of the polymer can be affected by both the temperature and salinity of the oil reservoirs (Muller et al., 1980; Seright et al., 2010; Al-Sabagh et al., 2016). Temperature and salinity affect PAM viscosity differently. Higher temperatures reduce viscosity by increasing polymer solubilization (Pramanik et al., 2017). Rheology is best explained as the study of deformation or flow behavior under applied stress (Temraz and Hassanien, 2016). Many principles are affected by pipe sticking, which depends on the rheology of the drilling fluid (Shakib et al., 2016). Khalil et al. examined the viscoplastic behavior of a liquid that penetrates biopolymers. The results demonstrated that the assortment technique can accurately predict the rheological response to these liquids' actions (Bourgoyne et al., 1986; Abduo MI. et al., 2016). As a unit that demonstrates the thixotropic feature, the gel strength is expressed as heads or tails (Seright et al., 2010). Because of the strong particles' mechanical grinding, plastic thickness is also known as the liquid's mechanical obstruction (Bingham, 1922). Yield strength, a limitation of Bingham's plastic model, is the crucial stream security attained by electrochemical reactions between mud particles that penetrate (Herschel and Bulkley, 1926). Using the Bingham model, the rheological limits of all exhausting fluids, including plasticity and apparent consistency, yield strength, and gel strength, are still a mystery. The American Oil Foundation (programming connection point) utilized the accompanying conditions to decide the rheological limits, which included AV, PV, and YP, as per the Bingham plastic model. The Bingham plastic model does not fully settle sensible consistency, plastic thickness, or yield attestation.

3.2.1 Determination of apparent viscosity

$$AV = \frac{\tau}{\gamma} = \frac{5,1.L.00}{1020} \quad P,$$

" A = 0.5 wt.% NPs "   "B = 1 wt. % NPs "   " C = 1.5wt% NPs "   " D = 2wt% NPs "   " E =2.5wt% NPs "   " F =3 wt.% NPs "

FIGURE 3
Mud cake with different concentrations of iron oxide(Fe$_2$O$_3$) nanoparticles (A−F).

TABLE 1 Mud cake formulation.

Constituent	Remark	Concentration
Freshwater	Based fluid	350 mL
Bentonite (g)	An organophilic clay	23
Barite (g)	Weighting agent	17
Carboxyl methyl cellulose (CMC) (g)	Fluid loss additive	2
Potassium chloride (KCl) (g)	Water activity and density	2 and 5
Anionic acrylic(g)	Viscosity control agent	2.5
Caustic soda (g)	pH control	0.6

$$AV = \frac{\tau}{\gamma} = \frac{5, 1.L.00}{1020} \quad P,$$

$$AV = \frac{L600}{2} \quad c.$$

Here, τ is the shear stress in [Pa]. L600 is the OFITE reading at 600 rpm, and 1,020 s-1 is the shear speed corresponding to the reading at 600 rpm.

3.2.2 Determination of plastic viscosity

$$PV = tg\alpha = \frac{\tau 2010 - \tau 510}{\gamma 600 - \gamma 300}.$$

3.2.3 Determination of yield point
From the Bingham plastic model, we have

$$\tau = PV.\gamma + YP = \; > YP = \tau - PV.\gamma,$$

$$YP = YP = \tau - 1020 \quad \frac{\tau 1020 - \tau 510}{1020 - 510}.1020$$

$$= 0, 511\,[L600 - 2\,(L600 - L300)],$$

$$YP = 0, 511.\,(2.L300 - L600) = 0, 511[L300 - \,(L600 - L300)],$$

$$YP = 0, 511.\,(L300 - PV),$$

$$We\;have\;1lb/100\,ft2 = 0.4788\,Pa,$$

$$YP = \frac{0.511\,(L300 - PV)}{0.4788},$$

$$1, 067.\,(L300 - VP) \sim YP = L300 - VP\left[\frac{11lb}{100\,ft2}\right].$$
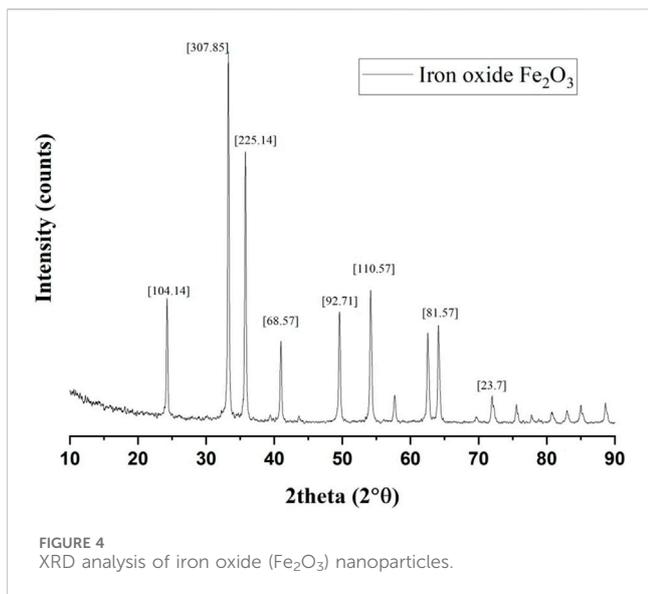
Here, YP is the yield point, PV is the plastic viscosity, and γ is the shear rate or strain rate; to find the shear stress (τ), do the following:

- For pascal, multiply the OFITE readings by 0.511.
- For deca pascal, multiply the OFITE readings by 5.11.
- For milli pascal, multiply the OFITE readings by 511.
- For pounds per 100 square feet, multiply the readings by 1.067.

3.3 Standard error

The limit of any explanatory model laid out to facilitate the nonlinear backslide at a high shear rate will describe its accuracy. As this limit shifts with each logical articulation, the determined rheological boundaries offer unmistakable qualities for different models. The standard error for each rheological model has been determined using Eq. (1) (Papanastasiou, 1987). At last, the best-fitted and most successful demonstration was determined.

$$SE = \frac{1000^*\left[\frac{\sum(measured\;value - calculated\;value)^{1/2}}{(number\;of\;data\;points - 2)}\right]}{(\boldsymbol{Maximum}\;measured\;value\; - \;Minimum\;measured\;value)}.$$

(1)

FIGURE 4
XRD analysis of iron oxide (Fe$_2$O$_3$) nanoparticles.

TABLE 2 Physical properties of Fe$_2$O$_3$ NPs.

Property	Typical value
Purity	99.90%
Appearance	Red powder
Size	20–30 nm
Ash	>0.21wt%

4 Results and analysis

4.1 Characteristics of iron oxide (Fe$_2$O$_3$) nanoparticles

4.1.1 XRD of iron oxide (Fe$_2$O$_3$) nanoparticles

The X-ray powder diffraction pattern of the synthesized iron oxide (Fe$_2$O$_3$) nanoparticles is shown in Figure 4. The XRD analysis of synthesized NPs demonstrates the characteristic pattern of α-Fe$_2$O$_3$. The characteristic peaks appear in the following 2θ ranges: ≈24.150, 33.760, 36.250, 42.340, 50.120, 54.20, 64.900, and 72.650, which correspond to 104.14, 307.85, 225.14, 68.57. 92.72, 110.57, 81.57, and 23.7, respectively. From the Debye–Scherrer formula, D = Kλβcosθ, the crystal size of the synthesized iron nanoparticle was computed to be approximately 40 nm. From XRD analysis, the crystallinity of synthesized NPS was found to be 75.46%.

### 4.1.2 Physical description of iron oxide (Fe$_2$O$_3$) nanoparticles

Iron oxide nanoparticles, Fe$_2$O$_3$, are composed of iron and oxygen atoms and are characterized by their distinct appearance and properties that differentiate them from bulk iron oxide materials. These nanoparticles typically have diameters ranging from 1 to 100 nm, making them thousands of times smaller than a human hair. As a result of their small size, they exhibit unique properties and behaviors compared to their bulk counterparts. The physical description of Fe$_2$O$_3$ nanoparticles emphasizes their small size, unique colors, and magnetic properties, which make them a fascinating and versatile material with numerous potential applications across various fields. In Table 2, we present the physical properties of the iron oxide used in our experiments, including a particle size of 30 nm, a specific surface area of 37 m̎2/g, and a bulk density of 0.21 g/cm̎3.

4.1.3 Scanning electron microscopy (SEM) of iron oxide (Fe$_2$O$_3$) and mud cake E

For the iron oxide SEM (Figure 5), we used a small quantity of already synthesized iron oxide. In addition, we employed the Thermo

FIGURE 5
SEM of iron oxide (Fe$_2$O$_3$).

FIGURE 6
SEM of mud cake E.
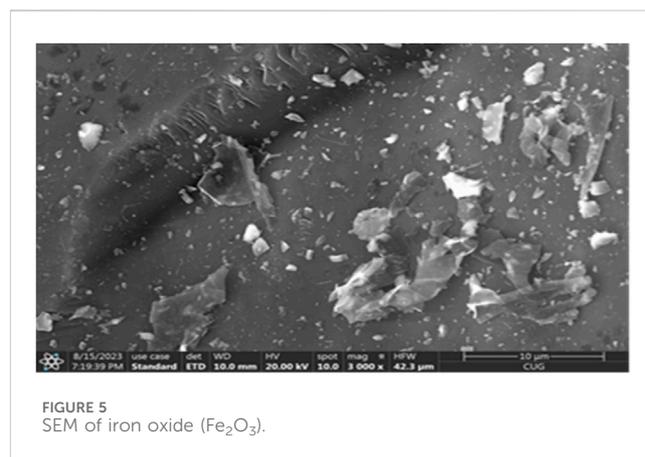
Fisher Scientific Apreo Scanning Electron Microscope to perform elemental analysis of the iron oxide. SEM was performed at 5,000 × magnification. According to the SEM (Figure 6), we notice that the grains are in the form of clusters, each grain is in the form of flowers in assembly, and we can observe that the SEM of the mud cake E is characterized by large components in the form of bubbles, primarily advantageous for fluid loss control, and a magna in assembly.

4.2 Impact of iron oxide on the plastic viscosity

In terms of how the iron oxide, nano Fe$_2$O$_3$, nanoparticles affect the consistency of the plastic, we discovered that the number of
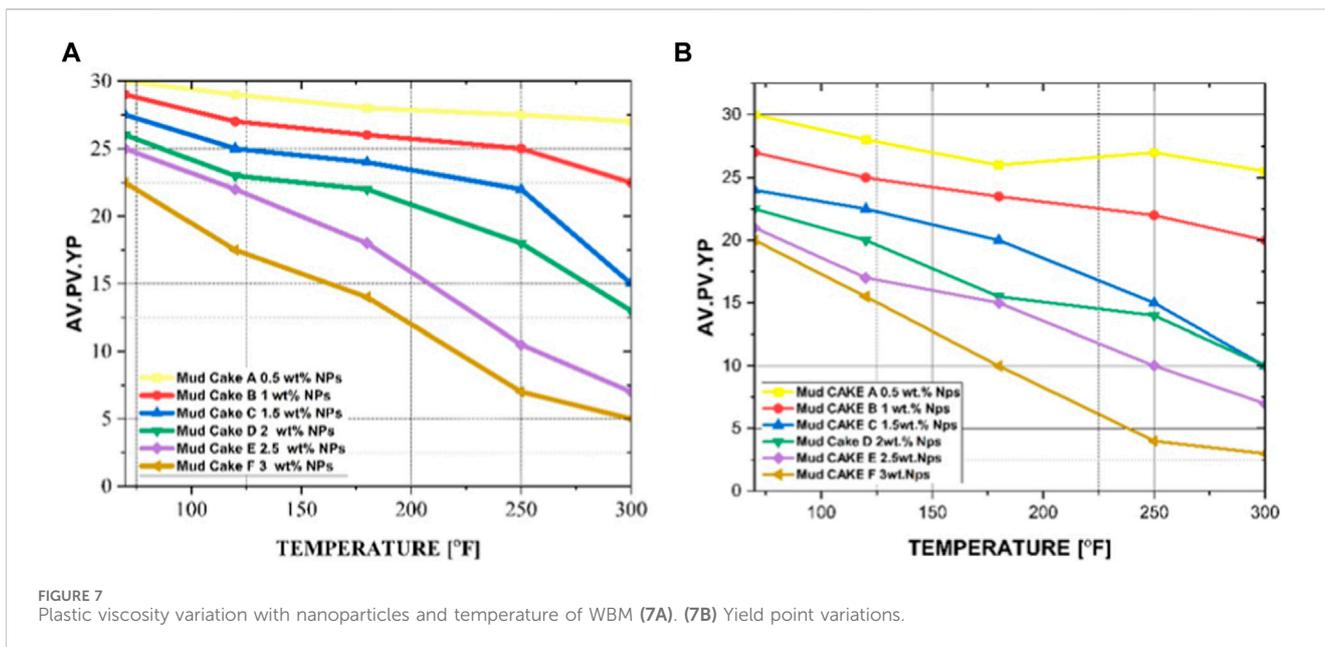
FIGURE 7
Plastic viscosity variation with nanoparticles and temperature of WBM **(7A)**. **(7B)** Yield point variations.

TABLE 3 Plastic viscosity variation under temperature and nano Fe_2O_3.

T mud cake	70°F	120°F	180°F	250°F	300°F
Mud cake A	30	28	27	27	25.5
Mud cake B	27	25	23	22	20
Mud cake C	24	22.5	20	15	10
Mud cake D	22.5	20	15.5	14	10
Mud cake E	21	17	15	10	7
Mud cake F	20	15	10	4	2

nanoparticles increases and decreases in tandem with temperature and that the plastic thickness increases effectively. To bring rock shavings to the surface, PV with nanoparticle fixation ascends and chips away at the liquid's entry restriction, especially in large apertures where the siphon's annular speed is relatively small (Casson, 1959). This is the result of the solid rate increasing and the size of the important solid areas decreasing. According to assessments conducted by Yahia and Khayat (2001), differentiation appears to be the particles or a combination of them, and the plastic's thickness is developing in light of the presence of nanoparticles in WBM. The results showed a pattern. Mud cake A was inspected at a pressure of 10,000 psi and a temperature of 300°F. As demonstrated in Figure 7 and Table 3, we discover a significant reduction of 88.10% of WBM PV with an exceptionally low fraction of nanoparticles about the nano effect on the plastic thickness of the water-based mud. Debris will be less flexible and more likely to stick behind the drill head and come out of the slurry, which will make drilling impossible. Nevertheless, with the addition of nanoparticle blends of 2.5 weight percent NPs and 3 weight percent NPs, a reduction of 14.77% PV was seen at high temperatures of 300°F and pressures of 10,000 psi. Exceptionally high PV proportions can be reduced by adjusting ownership limits, avoiding extremely high consistency and siphon tension, separating excess solids, and implementing incapacitation measures. There is a

2.7 YP–PV extent. It displays the drilling fluid's speed profile as it passes through the annulus or space created between a drill pipe and the penetrated wall. A greater YP–PV extent results in a thicker profile, which is necessary for the slurry to move, cutting clearance (Ahmad et al., 2017). In addition, a high (YP–PV) ratio or a low n value allows better cutting transport and better hole cleaning (Samaei and Tahmasbi, 2007).

4.3 Thermal impact of iron oxide (Fe_2O_3) on the yield point

The range of YP that affects iron oxide nanoparticles under high strain and temperature conditions is displayed in Figure 8B and Table 4. The centralization of nanoparticles causes a global decrease in temperature that is below the expectations of many. Changes in the liquid solids' surface properties, their centralization and electrical arrangement, and the kinds and fixation of particles in the liquid phase of the borehole as the association of nanoparticles expands are the causes of these variations in yield strength.

4.4 Effect of nano Fe_2O_3 on gel strength variation under HPHT

Tables 5 and 6 and Figures 8A,B show that the iron oxide size is 0.5 weight percent. At 300°F and 10,000 psi of strain, mud cake A showed a significant decrease in WBM and YP of 76.60%. Drill cuttings are essentially affected in significant areas of strength by this reduction. The assessment of the impact of iron oxide nanoparticles on the rheological properties of water-based mud in a high-temperature, high-strain (HPHT) environment and the proper well restoration during crippling conditions (Okrajni and Azar, 1986). Nonetheless, compared to thermally settled samples, the WBM increases by 2.5 weight percent. Under comparable HPHT conditions, NPs only experience a 9.57 percent decrease in the yield limit.
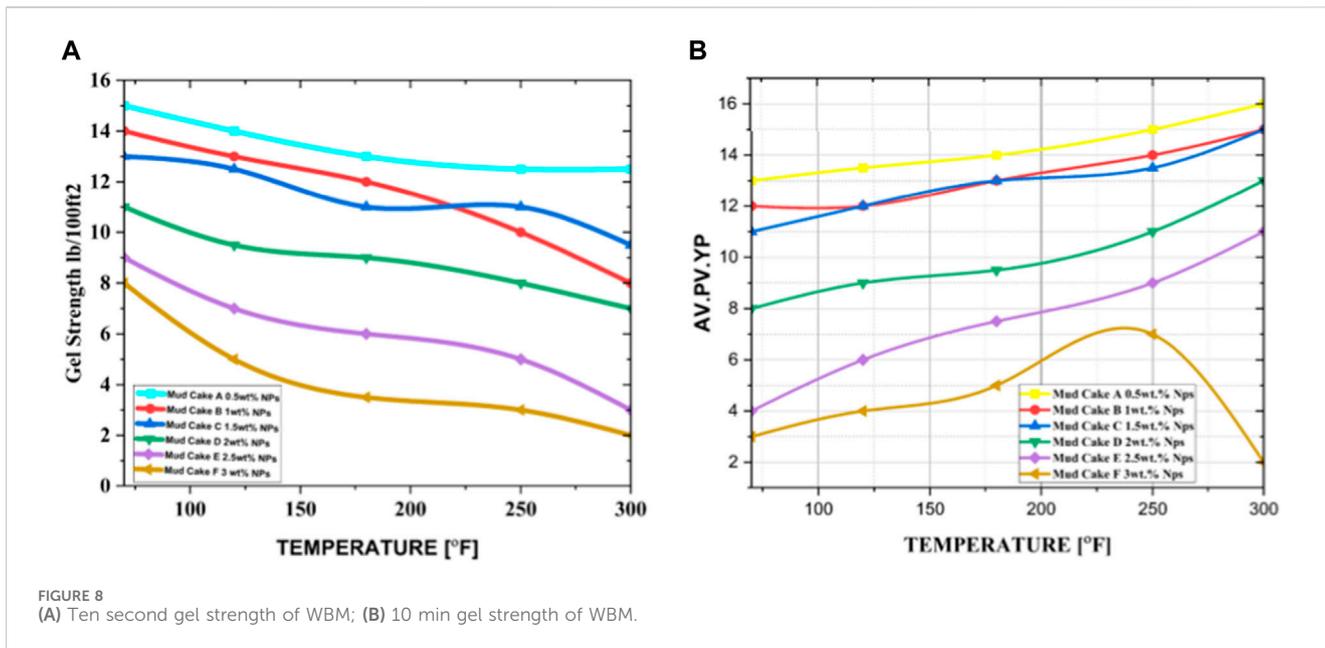
FIGURE 8
(A) Ten second gel strength of WBM; **(B)** 10 min gel strength of WBM.

TABLE 4 Yield point variation under temperature and nano Fe_2O_3.

T mud cake	70°F	120°F	180°F	250°F	300°F
Mud cake A	30	29	28	27.5	27
Mud cake B	29	27	26	25	22.5
Mud cake C	27.5	25	24	22	15
Mud cake D	26	23	22	18	13
Mud cake E	25	22	18	10.5	7
Mud cake F	22.5	17.5	14	7	5

TABLE 6 Ten-minute gel strength under temperature and nano Fe_2O_3.

T mud cake	70°F	120°F	180°F	250°F	300°F
Mud cake A	13	13.5	14	15	16
Mud cake B	12	12	13	14	15
Mud cake C	11	12	13	13.5	15
Mud cake D	8	9	9.5	11	13
Mud cake E	4	6	7.5	9	11
Mud cake F	3	4	5	7	2

TABLE 5 Ten-second gel strength variation under temperature and nano Fe_2O_3.

T mud cake	70°F	120°F	180°F	250°F	300°F
Mud cake A	15	14	13	12.5	12.5
Mud cake B	14	13	12	10	8
Mud cake C	13	12.5	11	11	9.5
Mud cake D	11	9.5	9	8	7
Mud cake E	9	7	6	5	3
Mud cake F	8	5	3.5	3	2

5 Analysis of shear stress *versus* shear rate variation under HPHT

The stream lead's sign indicates a liquid's propensity to shear when subjected to strain and temperature changes. Shear pressure analysis has demonstrated that as nanoparticle concentration increases, so does the liquid's growth due to shear (refer to Figures 9A–F). Due to the high heat and strains, mud cake A was subsequently reduced, and the garbage structure as a whole experienced a high-shear, low-fat composition. In any case, as the concentration of nanoparticles increases to the ideal combination of 2.5 weight percent NPs, the liquid structure demonstrates its thermal stability. According to the results obtained from Table 7, Table 8, Table 9, Table 10, Table 11, Table 12, when the temperature increases, the shear stress *versus* rate changes rapidly, and from this, we can deduce that the temperature and pressure influence the shear stress *versus* rate.

6 Effect of nano Fe_2O_3 on the rheology behavior of drilling muds

The estimation of the rheology of drilling muds in the Dibella oil field exhibits a shear-thinning behavior, which demonstrates that an increase in the shear rate causes a decrease in consistency, as displayed in Figure 10. According to Figure 10, the plastic viscosity initially remains unchanged at a low concentration of NPs. However, at higher concentrations, plastic viscosity improves. Specifically, mud cake B with a
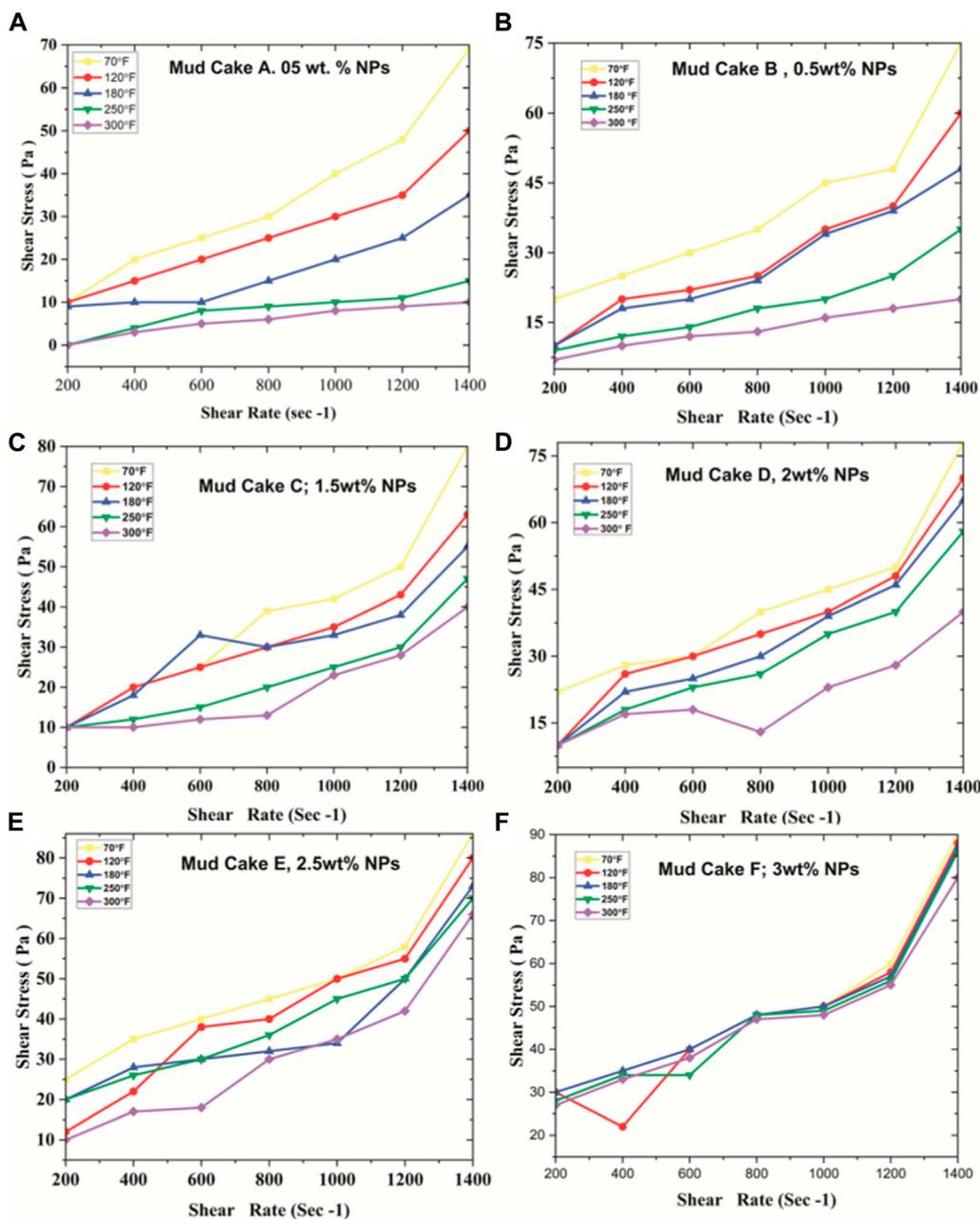
FIGURE 9
Shear stress *versus* shear rate variant with temperature for mud cake **(A—F)**.

concentration of 1 wt% shows a 10% improvement in plastic viscosity compared to mud cake A at 0.5 wt%. Additionally, mud cake F with 3 wt% NP demonstrates an approximately 30% increase in plastic viscosity. The increase in plastic viscosity can be attributed to the presence of NPs, which contribute to the overall dispersed solids in the sludge system. A low shear rate builds the iron oxide nanoparticle focus and shows higher consistency compared with a low nanoparticle rate mud; it uncovers a significant property of the penetrating liquid, as high viscosities are fundamental under static circumstances and low viscosities are necessary under conditions to

eliminate cuttings from the lower part of the opening (Anawe et al., 2014). [77].

7 Effect of nano Fe$_2$O$_3$ on API fluid loss

The impact of nano Fe$_2$O$_3$ concentrations on fluid loss is illustrated in Figure 11. For all NP concentrations, the API fluid loss is reduced compared to the base mud, demonstrating the significant capability of NPs to control fluid loss. In the case of the base mud, mud cake A yields 6 mL of filtrate in the 30-min API

TABLE 7 Shear stress *versus* shear rate variation with temperature mud cake A.

T τ	70°F	120°F	180°F	250°F	300°F
τ_{1400}	69	50	35	15	10
τ_{1200}	48	35	25	11	9
τ_{1000}	40	30	20	10	8
τ_{800}	30	25	15	9	6
τ_{600}	25	20	10	8	5
τ_{400}	20	15	10	4	3
τ_{200}	10	10	9	0	0

TABLE 10 Shear stress *versus* shear rate variation with temperature for mud cake D.

T τ	70°F	120°F	180°F	250°F	300°F
τ_{1400}	80	70	65	58	40
τ_{1200}	50	48	46	40	28
τ_{1000}	45	40	39	35	23
τ_{800}	40	35	30	26	13
τ_{600}	30	30	25	23	18
τ_{400}	28	26	22	18	17
τ_{200}	22	10	10	10	10

TABLE 8 Shear stress *versus* shear rate variation with temperature for mud cake B.

T τ	70°F	120°F	180°F	250°F	300°F
τ_{1400}	75	60	48	35	20
τ_{1200}	48	40	39	25	18
τ_{1000}	45	35	34	20	16
τ_{800}	35	25	24	18	13
τ_{600}	30	22	20	14	12
τ_{400}	25	20	18	12	10
τ_{200}	20	10	10	9	7

TABLE 11 Shear stress *versus* shear rate variation with temperature for mud cake E.

T τ	70°F	120°F	180°F	250°F	300°F
τ_{1400}	86	80	73	70	66
τ_{1200}	58	55	50	50	42
τ_{1000}	50	50	34	45	35
τ_{800}	45	40	32	36	30
τ_{600}	40	38	30	30	18
τ_{400}	35	22	28	26	17
τ_{200}	25	12	20	20	10

TABLE 9 Shear stress *versus* shear rate variation with temperature for mud cake C.

T τ	70°F	120°F	180°F	250°F	300°F
τ_{1400}	78	63	55	47	40
τ_{1200}	50	43	38	30	28
τ_{1000}	42	35	33	25	23
τ_{800}	39	30	30	20	13
τ_{600}	25	25	33	15	12
τ_{400}	20	20	18	12	10
τ_{200}	10	10	10	10	10

TABLE 12 Shear stress *versus* shear rate variation with temperature for mud cake F.

T τ	70°F	120°F	180°F	250°F	300°F
τ_{1400}	90	88	87	86	80
τ_{1200}	60	58	57	56	55
τ_{1000}	50	50	50	49	48
τ_{800}	48	48	48	48	47
τ_{600}	40	40	40	34	38
τ_{400}	35	22	35	34	33
τ_{200}	30	30	30	28	27

filter test. On the other hand, mud cake B with an NP concentration of 1 wt% produces 5.3 mL of filtrate, representing a 12.4% improvement in fluid loss control compared to mud cake A. Experimental observation reveals that the cumulative fluid loss is minimized (5.3 mL) at an NP concentration of 1 wt%. At higher NP concentrations, the cumulative fluid losses are slightly higher (6–4.5 mL), confirming the optimal performance of hematite nanoparticles at a concentration of 2.5 wt%. This value aligns closely with the findings of previous experimental work. In conclusion, it can be inferred that a concentration of 2.5 wt% provides a sufficient quantity of NPs to block the pore space of the filter paper. At higher concentrations, the volume of NPs relative to other additives increases, which affects the formation of a proper bridge and results in a slight increase in filtrate volume.

8 Conclusion

The effects of the addition of iron oxide solutions were investigated using rheological, chemical, and thermal analyses. The following outcomes can be drawn based on the results obtained:

1. Under HPHT conditions, the concentration of iron oxide increases plastic viscosity, yield strength, and gel strength.

FIGURE 10
Effect of iron oxide nanoparticle on viscosity at different shear rates.

FIGURE 11
Comparison of total fluid loss between drilling muds after 30 min.
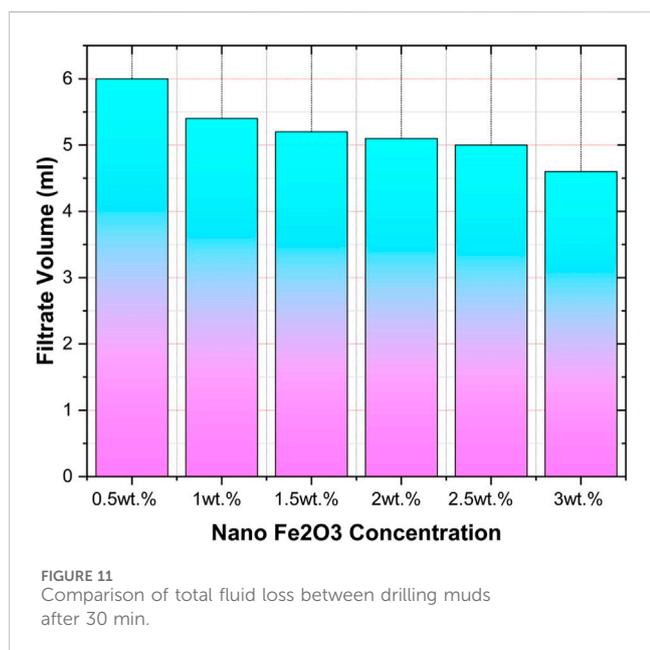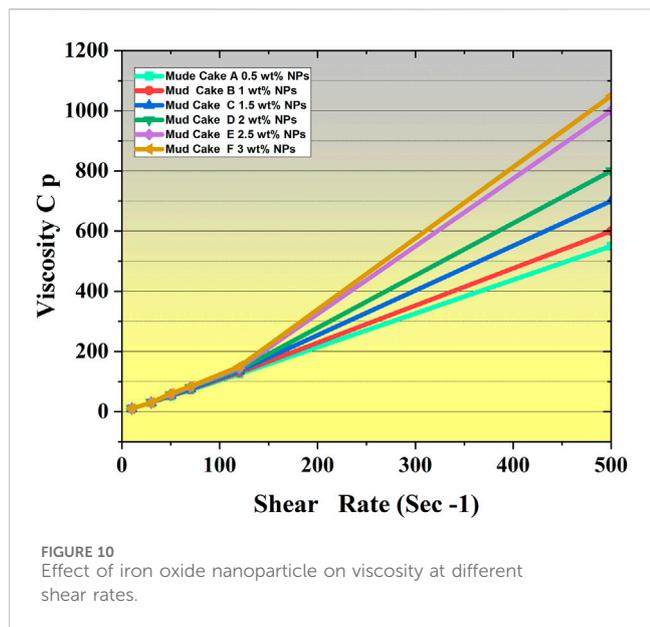
However, the expansion remains within an acceptable range for optimal water execution.

2. A combination of 2.5% weight percent iron nanoparticles helps maintain highly and thermally stable rheological properties under 300°F and 10,000 pressure. There is a slight drop in gel strength of 14.77%, 9.57%, 14.77%, and 16.58%. After 16 h of hot rolling, mud cake E, which includes 2.5% weight percent NPs, maintains a high YP–PV ratio of 2.7.

3. Hematite Fe_2O_3 helps achieve a liquid design that is neither excessively restricted nor overly thick at high temperatures. It controls the consistency collection speed with the shear change speed. The effects of iron oxide nanoparticles on the rheological properties of water-based mud are examined under high stresses in an HPHT scenario.

4. As nanocomposite items grew, the thickness of the channel cake and fluid incident decreased. Rheology testing and SEM analysis of the mud showed that iron oxide mud (mud E), containing 2.5% weight percent iron oxide, permits the use of anionic acrylic as a loss circulation material up to 300°F. It has satisfactory rheological and liquid-loss properties. Iron oxide drilling fluid with anionic acrylic has excellent stability and sealing capabilities at high temperatures, making it a suitable option for high-temperature, high-pressure wells with loss of circulation.

5. At 1 wt%, NP concentration reduces fluid loss to 5.3 mL and mud cake thickness by 40% compared to mud cake A. Slightly higher NP concentrations (6–4.5 mL) still perform optimally.

Data availability statement

The original contributions presented in the study are included in the article/Supplementary Material; further inquiries can be directed to the corresponding author.

Author contributions

Funding

Conflict of interest

The authors declare that the research was conducted in the absence of any commercial or financial relationships that could be construed as a potential conflict of interest.

Publisher's note

All claims expressed in this article are solely those of the authors and do not necessarily represent those of their affiliated organizations, or those of the publisher, the editors, and the reviewers. Any product that may be evaluated in this article, or claim that may be made by its manufacturer, is not guaranteed or endorsed by the publisher.

References

Aadnoy, B. S., and Chenevert, M. E. (1987). Stability of highly inclined boreholes. *SPE Drill. Eng.* 2 (4), 364–374. doi:10.2118/16052-pa

Abdo, J., and Haneef, M. (2012). Nano-enhanced drilling fluids: pioneering approach to overcome uncompromising drilling problems. *J. Energy Resour. Technol.* 134 (1). doi:10.1115/1.4005244

Abdo, J., and Haneef, M. D. (2013). Clay nanoparticles modified drilling fluids for drilling of deep hydrocarbon wells. *Appl. ClaySci.* 86, 76–82. doi:10.1016/j.clay.2013.10.017

Abdo, J., Zaier, R., Hassan, E., Alsharji, H., and AlShabibi, A. (2014). ZnO-clay nano-composites forenhanceddrillingatHTHPconditions. *Surf. InterfaceAnal.* 46 (10–11), 970–974. doi:10.1002/sia.5454http://onlinelibrary.wiley.com/doi/10.1002/sia.5454/abstract

Abduo, M. I, Dahab, A. S., Abuseda, H., AbdulAziz, A. M., and Elhossieny, M. (2016a). Comparative study of using water-based mud containing multiwall carbon nanotubes versus oil-based mud in HPHT fields. *Egypt. J. Petroleum* 25 (4), 459–464. doi:10.1016/j.ejpe.2015.10.008

Abduo, M. I, Dahab, A. S., Abuseda, H., AbdulAziz, A. M., and Elhossieny, M. S. (2016b). Comparative study of using water-basedmudcontainingmultiwallcarbonnanotubesversus oil-based mudinHPHT fields. *Egypt. J. Pet.* 25, 459–464. doi:10.1016/j.ejpe2015.10.008

Ahmad, H. M., Kamal, M. S., and Murtaza, M., Improving the drilling fluid properties using nanoparticles and water-soluble polymers[C]//SPE Kingdom of Saudi Arabia annual technical symposium and exhibition. OnePetro, Richardson, TX, USA, 2017.

Akhtarmanesh, S., Shahrabi, M. J. A., and Atashnezhad, A. (2013). Improvement of wellbore stability in shale using nanoparticles. *J. Petroleum Sci. Eng.* 112, 290–295. doi:10.1016/j.petrol.2013.11.017

Al-Saba, M. T., Al Fadhli, A., and Marafi, A., Application of nanoparticles in improving rheological properties of water-based drilling fluids[C]//SPE Kingdom of Saudi Arabia Annual technical symposium and exhibition. SPE, Lumpur, Malaysia, 2018: SPE-192239-MS.

Al-Sabagh, A. M., Kandile, N., El-Ghazawy, R., Noor El-Din, M., and El-Sharaky, E. (2016). Solution properties of hydrophobically modified polyacrylamides and their potential use for polymer flooding application. *Egypt. J. Pet.* 25, 433–444. doi:10.1016/j.ejpe.2015.03.014

Al-Yasiri, M. S., and Al-Sallami, W. T. (2015). How the drilling fluids can be made more efficient by using nanomaterials. *Am. J. Nano Res. Appl.* 3 (3), 41–45.

Anawe, P. A. L., Efeovbokhan, V. E., and Ayoola, A. A., (2014). Investigating alternatives to diesel in oil-based drilling mud formulations used in the oil industry. *J. Environ. Earth Sci.* 4 (14), 70–77. challenges", Houston https://www.aade.org/application/files/7515/7304/4596/AADE-03-NTCE-40-Fraser.pdf.

Aramendiz, J., and Imqam, A. (2019). Water-based drilling fluid formulation using silica and graphene nanoparticles for unconventional shale applications. *J. Pet. Sci. Eng.* 179, 742–749. doi:10.1016/j.petrol.2019.04.085

Bayat, A. E., and Shams, R. (2019). Appraising the impacts of SiO2, ZnO and TiO2 nanoparticles on rheological properties and shale inhibition of water-based drilling muds. *Colloids Surf. A* 581, 123792. doi:10.1016/j.colsurfa.2019.123792

Bingham, E. C. (1922). *Fluidity and plasticity*. New York, NY, USA: McGraw-Hill Book Company.

Bourgoyne, A. T., Millheim, K. K., and Chenevert, M. E., *Applied drilling engineering*. Society of Petroleum Engineers London, UK, 1986.

Brady, J. F., and Brady, J. F. (1983). The Einstein viscosity correction in dimensions. *Int. J. Multiph. flow* 10 (1), 113–114. doi:10.1016/0301-9322(83)90064-2

Caenn, R., Darley, H. C. H., and Gray, G. R. *Composition and properties of drilling and completion fluids*[M]. Gulf Professional Publishing, Houston, TX, USA, 2011.

Casson, N. (1959). *A flow equation for pigment-oil suspensions of the printing ink type*. Oxford, UK: Pergamon Press

Cheraghian, G., Khalili Nezhad, S. S., Kamari, M., Hemmati, M., Masihi, M., and Bazgir, S., (2015). Effect of nanoclay on improved rheology properties of polyacrylamide solutions used in enhanced oil recovery. *J. Pet. Explor. Prod. Technol.* 5, 189–196. doi:10.1007/s13202-014-0125-y

Christiansen, C.,1991.Fromoil-basedmudtowater-basedmud.In: Proceedings of the 1991SPEHealth, SafetyandEnvironmentinOilandGasExplorationand Production 11–14 November, TheHague, Netherlands, pp.1–9. doi:10.2118/23359-MS

Coussot, P., Bertrand, F., and Herzhaft, B. (2004). Rheological behavior of drilling muds, characterization using MRI visualization. *Oil gas Sci. Technol.* 59 (1), 23–29. doi:10.2516/ogst:2004003

Du, S., Wu, J., AlShareedah, O., and Shi, X. (2019). Nanotechnology in cement-based materials: a review of durability, modeling, and advanced characterization. *Nanomaterials* 9 (9), 1213. doi:10.3390/nano9091213

Esmaeili, A., Patel, R. B., and Singh, B. P. (2011). Applications of nanotechnology in oil and gas industry. *AIP Conf. Proc.*, 133–136.

Ezell, R., and Harrison, D. J. Design of improved high-density, thermally-stable drill-in fluid for HTHP applications[C]//SPE Annual Technical Conference and Exhibition?. SPE, Lumpur, Malaysia, 2008: SPE-115537-MS.

Fakher, S., Ahdaya, M., and Imqam, A. (2020). Hydrolyzed polyacrylamide–Fly ash reinforced polymer for chemical enhanced oil recovery: Part 1–Injectivity experiments. *Fuel* 260, 116310. doi:10.1016/j.fuel.2019.116310

Gbadamosi, A. O., Junin, R., Manan, M. A., Agi, A., Oseh, J. O., and Usman, J. (2019). Synergistic application of aluminium oxide nanoparticles and oilfield polyacrylamide for enhanced oil recovery. *J. petroleum Sci. Eng.* 182, 106345. doi:10.1016/j.petrol.2019.106345

Geehan, T., Dudleson, W. J., Boyington, W. H., et al. Incentive approach to drill fluids management: an experience in central North sea[C]//SPE/IADC Drilling Conference. OnePetro, Richardson, TX, USA, 1989.

Godson, L., Raja, B., Lal, D. M., and Wongwises, S. (2010). Enhancement of heat transfer using nanofluids—an overview. *Renew. Sustain. energy Rev.* 14 (2), 629–641. doi:10.1016/j.rser.2009.10.004

Hamed, S. B., and Belhadri, M. (2009). Rheological properties of biopolymers drilling fluids. *J. Petroleum Sci. Eng.* 67 (3-4), 84–90. doi:10.1016/j.petrol.2009.04.001

Haruna, M. A., Nourafkan, E., Hu, Z., and Wen, D. (2019). Improved polymer flooding in harsh environments by free-radical polymerization and the use of nanomaterials. *Energy & Fuels* 33 (2), 1637–1648. doi:10.1021/acs.energyfuels.8b02763

Herschel, W., and Bulkley, R. (1926). Measurement of consistency as applied to rubber-benzene solutions. *Am. Soc. Test. Proc.*, 621–633.

Hu, Z., Haruna, M., Gao, H., Nourafkan, E., and Wen, D. (2017). Rheological properties of partially hydrolyzed polyacrylamide seeded by nanoparticles. *Ind. Eng. Chem. Res.* 56, 3456–3463. doi:10.1021/acs.iecr.6b05036

Ismail, A. R., Aftab, A., Ibupoto, Z. H., and Zolkifile, N. (2016). The novel approach for the enhancement of rheological properties of water-based drilling fluids by using multi-walled carbon nanotube, nano silica, and glass beads. *J. Petroleum Sci. Eng.* 139, 264–275. doi:10.1016/j.petrol.2016.01.036

Jain, R., Mahto, V., and Sharma, V. P. (2015). Evaluation of polyacrylamide-grafted-polyethylene glycol/silica nanocomposite as potential additive in water based drilling mud for reactive shale formation. *J. Nat. Gas Sci. Eng.* 26, 526–537. doi:10.1016/j.jngse.2015.06.051

Khalil, M., and Mohamed Jan, B. (2012). Herschel-Bulkley rheological parameters of a novel environmentally friendly lightweight biopolymer drilling fluid from xanthan gum and starch. *J. Appl. Polym. Sci.* 124 (1), 595–606. doi:10.1002/app.35004

Khodja, M., Canselier, J. P., Bergaya, F., Fourar, K., Khodja, M., Cohaut, N., et al. (2010). Shaleproblemsandwater-based drilling fluid optimisationinthe Hassi MessaoudAlgerianoil field. *Appl. ClaySci.* 49 (4), 383–393. doi:10.1016/j.clay.2010.06.008

Khoshakhlagh, A., Nazari, A., and Khalaj, G. (2012). Effects of Fe2O3 nanoparticles on water permeability and strength assessments of high strength self-compacting concrete. *J. Mater. Sci. Technol.* 28 (1), 73–82. doi:10.1016/s1005-0302(12)60026-7

Laszlo, K., Tombacz, E., and Josepovits, K. (2001). Effect of activation on the surface chemistry of carbons from polymer precursors. *Carbon* 39 (8), 1217–1228. doi:10.1016/s0008-6223(00)00245-1

Le Guen, Y., Le Gouevec, J., Chammas, R., Gerard, B., Poupard, O., Van Der Beken, A., et al. (2009). CO2 storage: managing the risk associated with well leakage over long time scales. *Facil. Constr.* 4 (3), 87–96. doi:10.2118/116424-pa

Li, X., Jiang, G., Yang, L., Wang, K., Shi, H., Li, G., et al. (2019). Application of gelatin quaternary ammonium salt as an environmentally friendly shale inhibitor for water-based drilling fluids. *Energy fuels.* 33 (9), 9342–9350. doi:10.1021/acs.energyfuels.9b01798

Livescu, S. (2012). Mathematical modeling of thixotropic drilling mud and crude oil flow in wells and pipelines—a review. *J. Petroleum Sci. Eng.* 98, 174–184. doi:10.1016/j.petrol.2012.04.026

Ma, L., Luo, P., He, Y., Zhang, L., Fan, Y., and Jiang, Z. (2020). Improving the stability of multi-walled carbon nano-tubes in extremely environments: applications as nano-plugging additives in drilling fluids. *J. Nat. Gas. Sci. Eng.* 74, 103082. doi:10.1016/j.jngse.2019.103082

Mady, A., Mahmoud, O., and Dahab, A. S. (2020). Nanoparticle-based drilling fluids as promising solutions to enhance drilling performance in Egyptian oil and gas fields. *Int. J. Ind. Sustain. Dev.* 1 (1), 24–38. doi:10.21608/ijisd.2020.73471

Mahmoud, M., Mohamed, A., Kamal, M. S., Sultan, A., and Hussein, I. (2019). Upgrading calcium bentonite to sodium bentonite using seawater and soda ash. *Energy fuels.* 33 (11), 10888–10894. doi:10.1021/acs.energyfuels.9b02900

Mao, H., Qiu, Z., Shen, Z., and Huang, W. (2015a). Hydrophobic associated polymer based silica nanoparticles composite with core–shell structure as a filtrate reducer for drilling fluid at utra-high temperature. *J.Petrol.Sci. Eng.* 129, 1–14. doi:10.1016/j.petrol.2015.03.003

Mao, H., Qiu, Z., Shen, Z., and Huang, W. (2015b). Hydrophobic associated polymer based silica nanoparticles composite with core–shell structure as a filtrate reducer for drilling fluid at utra-high temperature. *J. Petroleum Sci. Eng.* 129, 1–14. doi:10.1016/j.petrol.2015.03.003

Mohamadian, N., Ghorbani, H., Wood, D. A., and Hormozi, H. K. (2018). Rheological and filtration characteristics of drilling fuids enhanced by nanoparticles with selected additives: an experimental study. *Adv. Geo-Energy Res.* 2 (3), 228–236. doi:10.26804/ager.2018.03.01

Mohammed, A. S. (2017). Effect of temperature on the rheological properties with shear stress limit of iron oxide nanoparticle modified bentonite drilling muds. *Egypt J. Pet.* 26, 791–802. doi:10.1016/j.ejpe.2016.10.018

Muller, G., Fenyo, J. C., and Selegny, E. (1980). High molecular weight hydrolyzed polyacrylamides. III. Effect of temperature on chemical stability. *J. Appl. Polym. Sci.* 25, 627–633. doi:10.1002/app.1980.070250409

Nagre, R. D., Zhao, L., and Owusu, P. A. (2014). Thermosaline resistant acrylamide-based polyelectrolyte as filtration control additive in aqueous-based mud. *Petroleum Coal* 56 (3).

Nasser, J., Jesil, A., and Mohiuddin, T., (2013). Experimental investigation of drilling fluid performance as nanoparticles. *World J. Nano Sci. Eng.* 3. 33008, doi:10.4236/wjnse.2013.33008

Nelson, E. B., Baret, J. F., and Michaux, M. 3 Cement additives and mechanisms of action [M]//*Developments in Petroleum science*. Elsevier, Amsterdam, Netherlands, 1990, 28: 1–37.

Nourafkan, E., Haruna, M. A., Gardy, J., and Wen, D. (2019). Improved rheological properties and stability of multiwalled carbon nanotubes/polymer in harsh environment. *J. Appl. Polym. Sci.* 136 (11), 47205. doi:10.1002/app.47205

Okrajni, S., and Azar, J. J. (1986). The effects of mud rheology on annular hole cleaning in directional wells. *SPE Drill. Eng.* 1 (04), 297–308. doi:10.2118/14178-PA

Papanastasiou, T. C. (1987). Flows of materials with yield. *J. rheology* 31 (5), 385–404. doi:10.1122/1.549926

Pramanik, C., Gissinger, J. R., Kumar, S., and Heinz, H. (2017). Carbon nanotube dispersion in solvents and polymer solutions: mechanisms, assembly, and preferences. *ACS Nano2017* 11, 12805–12816. doi:10.1021/acsnano.7b07684

Rana, A., Arfaj, M. K., Yami, A. S., and Saleh, T. A. (2020). Cetyltrimethylammonium modified graphene as a clean swelling inhibitor in water-based oil-well drilling mud. *J. Environ. Chem. Eng.* 8, 103802. doi:10.1016/j.jece.2020.103802

Rashad, A. M. (2013). Metakaolin as cementitious material: history, scours, production, and composition–A comprehensive overview. *Constr. Build. Mater.* 41, 303–318. doi:10.1016/j.conbuildmat.2012.12.001

Rezaei, A., Nooripoor, V., and Shahbazi, K. Applicability of Fe$_3$O$_4$ nanoparticles for improving rheological and filtration properties of bentonite-water drilling fluids in the presence of sodium, calcium, and magnesium chlorides. *J. Petroleum*, 10, 2453–2464 (2020). doi:10.1007/s13202-020-00920-6

Riley, M., Young, S., Stamatakis, E., Guo, Q., Ji, L., and DeStefano, G., 2012.Wellborestabilityinunconventionalshales—the design of nano-particle fluid. In: Proceedingsofthe2012SPEOilandGasIndiaConferenceand Exhibition, 28–30 March, Mumbai, India, pp.1–8. doi:10.2118/153729-MS

Rodrigues, J. d.A., Lachter, E. R., deS, C. H., deMello, M., and Nascimento, R. S. V. (2006). *Newmultifunctionalpolymericadditivesforwater-based muds*. SanAntonio, TX, USA: PaperPre- sented attheSPEAnnualTechnicalConferenceandExhibition. doi:10.2118/106527-STU

Sadeghalvaad, M., and Sabbaghi, S. (2015). TheeffectoftheTiO2/polyacrylamidenano-composite on water-based drilling fluid properties. *PowderTechnol* 272, 113–119. doi:10.1016/j.powtec.2014.11.032

Samaei, M. S., and Tahmasbi, K. (2007) The possibility of replacing oil-based mud with environmentally acceptable water-based glycol drilling mud for the Iranian fields. Paper presented at the SPE &P environmental and safety conference, Galveston, Texas, USA doi:10.2118/106419-ms

Seright, R. S., Campbell, A. R., Mozley, P. S., and Han, P. (2010). Stability of partially hydrolyzed polyacrylamides at elevated temperatures in the absence of divalent cations. *SPE J.* 15, 341–348. doi:10.2118/121460-pa

Shakib, J. T., Kanani, V., and Pourafshary, P. (2016). Nano-clays as additives for controlling filtration properties of water–bentonite suspensions. *J. Petroleum Sci. Eng.* 138, 257–264. doi:10.1016/j.petrol.2015.11.018

Sikora, P., Abd Elrahman, M., and Stephan, D. (2018). The influence of nanomaterials on the thermal resistance of cement-based Composites A review. *Nanomaterials* 8 (7), 465. doi:10.3390/nano8070465

Singh, L. P., Agarwal, S. K., Bhattacharyya, S. K., Sharma, U., and Ahalawat, S. (2011). Preparation of silica nanoparticles and its beneficial role in cementitious materials. *Nanomater. Nanotechnol.* 1, 9. doi:10.5772/50950

Taraghikhah, S., Kalhor Mohammadi, M., and Tahmasbi Nowtaraki, K. Multifunctional nano additive in water-based drilling fluid for improving shale stability[C]International petroleum technology conference. OnePetro, Richardson, TX, USA, 2015.

Tehrani, A., Young, S., Gerrard, D., and Fernandez, J.,2009.Environmentally friendly waterbased fluid forHT/HPdrilling.In:Proceedingsofthe2009SPEInterna- tional SymposiumonOilfield Chemistry,20–22 April, TheWoodlands, TX, USA,pp.1–8. doi:10.2118/121783-MS

Temraz, M. G., and Hassanien, I. (2016). Mineralogy and rheological properties of some Egyptian bentonite for drilling fluids. *J. Nat. Gas Sci. Eng.* 31, 791–799. doi:10.1016/j.jngse.2016.03.072

Vermolen, E., Menno Van Haasterecht, J. T., Shehadeh Masalmeh, K., Marinus Faber, J., Diederik Michiel, B., and Marc Gruenenfelder, A. (2011). Pushing the envelope for polymer flooding towards high-temperature and high-salinity reservoirs with polyacrylamide-based terpolymers. *Soc. Petroleum Eng.*, 2011, 141497.

Yahia, A., and Khayat, K. H. (2001). Analytical models for estimating yield stress of high-performance pseudoplastic grout. *Cem. Concr. Res.* 31, 731–738. doi:10.1016/s0008-8846(01)00476-8